

Wireless Synchronous Transfer of Power and Reverse Signals

Yang Li[†], Yumei Li^{*}, Shaojie Feng^{*}, Qingxin Yang^{*}, Weihao Dong^{*}, Jingtai Zhao^{*}, and Ming Xue^{*}

^{†,*}Tianjin Key Laboratory of Advanced Electrical Engineering and Energy Technology,
Tianjin Polytechnic University, Tianjin, China

Abstract

Wireless power transfer via coupled magnetic resonances has been a hot research topic in recent years. In addition, the number of related devices has also been increasing. However, reverse signals transfer is often required in addition to wireless power transfer. The structure of the circuit for a wireless power transfer system via coupled magnetic resonances is analyzed. The advantages and disadvantages of both parallel compensation and series compensation are listed. Then the compensation characteristics of the inductor, capacitor and resistor were studied and an appropriate compensation method was selected. The reverse signals can be transferred by controlling the compensation of the resistor. In addition, it can be demodulated by extracting the change of the primary current. A 3.3 MHz resonant frequency with a 100 kHz reverse signals transfer system platform was established in the laboratory. Experimental results demonstrate that wireless power and reverse signals can be transferred synchronously.

Key words: Coupled magnetic resonance, Reverse signals transfer, Synchronous, Wireless power transfer

I. INTRODUCTION

In recent years, the number of studies on wireless power transfer via coupled magnetic resonances has been increasing [1]-[5]. In addition, more and more applications are using wireless power transfer technology, such as electric vehicles, mobile phones and micro implantable medical sensors [6]-[8]. Wireless power transfer technology allows electrical equipment to be freed from jumbled lines, which greatly improves the mobility and safety of equipment [9].

In applications, wireless power transfer cannot be separated from signal transfer. Without cable connections, some signal information such as load temperature, battery charging state and personal identification, need to be transferred wirelessly.

Traditional wireless power and signal transfer methods mainly added signal transfer channels. In [10], apart from the initial power transfer channel, three signal transfer channels were added for bilateral signal transfer. In [11], a wireless

power and signal transfer system was designed and applied to a set of implantable medical devices. This system required signal coils, which indicates that the system received power and signals separately. In [12]-[15], the core structure of wireless power transfer was designed and optimized to reduce the interference between the power and signal transfers. Despite their higher accuracy and fast signal transfer speed, these methods required an extra pair of signal transfer coils, which increased the complexity of the whole transfer system, and were not conducive to product design [16]. At present, one of the advanced methods for power and signal transmission is to load the modulation signals to the power transfer coil so that the signals and power are simultaneously transferred in the same coil and received by the same receiving coil. Then the signals were extracted by a filtering and demodulation circuit and used for load monitoring, detecting, etc. This is referred to as wireless synchronous transfer of power and signals technology.

In [17], a dual-band resonance coupling power and signal transfer system was proposed, where the power transfer efficiency was improved to 70% when the load value was less than 10 Ω and the transmission distance was shorter than 120mm. In [18], the switching frequency of an inverter was changed according to different digital signals, which were

Manuscript received Jul. 9, 2018; accepted Nov. 6, 2018
Recommended for publication by Associate Editor Yijie Wang.

[†]Corresponding Author: liyang@tjpu.edu.cn
Tel: +86-158-22275770, Tianjin Polytechnic University

^{*}Tianjin Key Laboratory of Advanced Electrical Engineering and Energy Technology, Tianjin Polytechnic University, China

transferred by detecting the amplitude of the secondary side voltage. In [19], a phase-modulated transmission method was proposed by changing the secondary compensation capacitor. By changing the secondary compensation capacitor, the phase of the input voltage and the resonant current was changed and the signal was loaded. Based on reflected impedance, the method in [20] was implemented to regulate the capacity value of the secondary loop according to the transmitted signal. Then the current wave of the primary circuit was monitored to demodulate the signal. Until now, most of the studies on the wireless synchronous transfer of power and signals have been based on inductively coupled power transfer (ICPT) technology. There has been no research on the wireless synchronous transfer of power and reverse signals based on coupled magnetic resonances.

In the above methods, the wireless power and signals are transferred from the transmitter to the receiver. Since the information transfer needs interaction and feedback, it is important to transfer reverse signals from the receiving coil to the transfer coil. A new method for the wireless synchronous transfer of power and reverse signals based on coupled magnetic resonances is proposed in this paper. Note that during system operation, the signal transmission and power transmission were performed simultaneously in the same wireless channel. Firstly, the characteristics of the secondary side of the transfer system of the series and parallel compensation were studied. Then the advantages and disadvantages of the two compensation methods were compared. The characteristic of the secondary side of the transfer system compensation of the inductor, capacitor and resistor were studied, and a proper method for compensation was selected. Secondly, ASK was chosen as the modulation and demodulation method and a MOSFET switch circuit was designed for controlling the state of the compensation. Finally, a 3.3 MHz resonant frequency with a 100 kHz reverse signals transfer system was established, and the reverse signal can be transferred by detecting the change of the primary current.

II. SYSTEM STRUCTURE

A. Wireless Power Transfer via Coupled Magnetic Resonances

Existing wireless power transfer via coupled magnetic resonances is of a double-coil structure or a four-coil structure. The double-coil structure consists of a smaller number of coils. However, its resonance characteristics are susceptible to the power supply and load. Therefore, it needs to add compensation devices, which increases the instability and complexity of the system. The four-coil structure is composed of two single-turn coils and two multi-turn resonator coils. These two resonator coils can improve the efficiency and power transfer of the overall system. Since the resonator and the single coil do not contact each other, the coupling coefficient

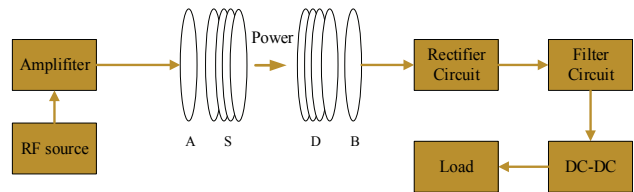


Fig. 1. Wireless power transfer system with a four-coil structure.

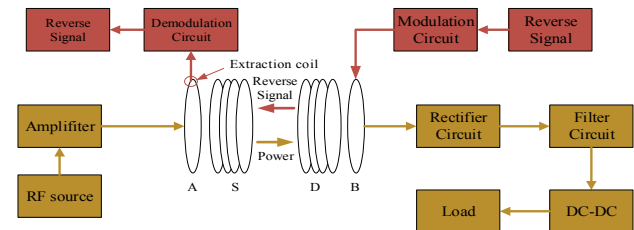


Fig. 2. Wireless synchronous transfer of power and reverse signals.

between them is small. The power transfer is mainly influenced by the value of Q . However, changes of load have little influence on the transfer of power. The stability of power transfer via coupled magnetic resonances can be enhanced by controlling the value of Q . Since the four-coil structure can keep the resonant state and power transfer stable, it was selected as the basic platform to study the transfer of coupled magnetic resonant wireless power and reverse signals [21].

Taking the four-coil structure as an example, the basic model of wireless power transfer via coupled magnetic resonances is shown in Fig. 1. The system consists of the following components: a radio frequency source (RF source), a transmitting coil A, a transmitter resonator S, a receiver resonator D, a receiving coil B and a load. The RF source provides a high-frequency signal for transmitting coil A. Then transmitting coil A transfers the power through self-oscillation. The power is transferred by electromagnetic coupling to the transmitter resonator S. Then the resonator D receives the power by a strong magnetic coupled resonance, and then transfers it to the receiving coil B. Finally, the receiving coil B provides power to the load.

B. Wireless Transfer of Power and Reverse Signals System

A system for the wireless transfer of power and reverse signals is shown in Fig. 2. It is implemented as follows. The RF source generates a sinusoidal signal of a desired resonant frequency. Then it is transferred through a signal amplifier. The power is transferred from the primary to the secondary side by the four-coil wireless power transfer structure. The received power is then sent through the rectifier circuit, filter circuit and DC-DC circuit successively. Thus, the load gets appropriate energy. The control of the compensation of the reverse signal is implemented by using the modulation circuit. The current of the primary coil changes due to the compensation. Thus, the change is extracted by the signal extraction coil, and the reverse signal can be obtained by the demodulation circuit.

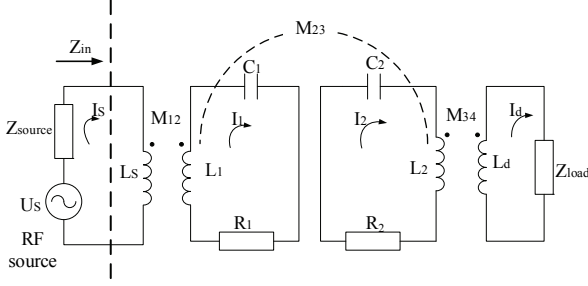


Fig. 3. Circuit model of a four-coil structure.

III. WORKING PRINCIPLE

A circuit model of a four-coil structure is shown in Fig. 3.

In a wireless power transfer via coupled magnetic resonance system, since the physical size of the coil is much smaller than the electromagnetic wavelength, energy is only transmitted in the near field, and only the coupling between adjacent coils needs to be considered. Therefore, only M_{12} , M_{23} and M_{34} are considered. According to KVL voltage equations, the following formulas are obtained.

$$\begin{cases} I_s Z_{source} - jI_s \omega L_s - jI_1 \omega M_{12} - U_s = 0 \\ I_1 \left(\frac{1}{j\omega C_1} + R_1 + j\omega L_1 \right) - jI_s \omega M_{12} - jI_2 \omega M_{23} = 0 \\ I_2 \left(\frac{1}{j\omega C_2} + R_2 + j\omega L_2 \right) - jI_1 \omega M_{23} - jI_d \omega M_{34} = 0 \\ I_d (j\omega L_d + Z_{load}) - jI_2 \omega M_{34} = 0 \end{cases} \quad (1)$$

where ω represents the angular frequency.

To make the two resonators have the exact same resonant frequency, the basic parameters are set the same. To simplify the calculation, the following transformations are carried out:

$$\begin{cases} Z = \frac{1}{j\omega C_1} + R_1 + j\omega L_1 = \frac{1}{j\omega C_2} + R_2 + j\omega L_2 \\ Z_s = j\omega L_s \\ Z_{12} = j\omega M_{12} \\ Z_{23} = j\omega M_{23} \\ Z_{34} = j\omega M_{34} \\ Z_d = j\omega L_d \end{cases} \quad (2)$$

Then the following formulas are obtained:

$$\begin{cases} U_s + I_s Z_s + I_1 Z_{12} - I_s Z_{source} = 0 \\ I_s Z_{12} - I_1 Z + I_2 Z_{23} = 0 \\ I_1 Z_{23} - I_2 Z + I_d Z_{34} = 0 \\ I_d Z_d + I_d Z_{load} - I_2 Z_{34} = 0 \end{cases} \quad (3)$$

In Fig. 3, U_s indicates the voltage of the RF source; L_s is the inductance of the excitation coil; Z_{source} is the impedance

of the RF source; Z_{in} is the input impedance of the four-coil structure wireless power transfer system; I_s is the current of the excitation circuit loop; I_d is the current of the load circuit loop; I_1 is the current of the transmitter resonant coil; I_2 is the current of the receiver resonant coil; M_{12} and M_{34} are the mutual inductances between the single turn coil and the multi-turn coils; L_1 and L_2 are the inductances of the transmitter resonator and the receiver resonators; C_1 and C_2 are the distributed capacitance transmitter and receiver resonators; R_1 and R_2 are the resistances of the transmitter and the receiver resonator; M_{23} is the mutual inductance between the resonators; L_d is the load coil inductance; and Z_{load} and the load impedance.

A further simplification is carried out as follows:

$$\begin{cases} I_d = \frac{I_2 Z_{34}}{Z_d + Z_{load}} \\ I_2 = \frac{Z_{23} (Z_{load} + Z_d) I_1}{Z Z_{load} + Z Z_d - Z_{34}^2} \\ I_1 = \frac{(Z Z_{12} Z_{load} + Z Z_{12} Z_d - Z_{12} Z_{34}^2) I_s}{Z (Z Z_{load} + Z Z_d - Z_{34}^2) - Z_{23}^2 (Z_{load} + Z_d)} \end{cases} \quad (4)$$

Formulas (4) can be substituted into (1). Thus, Z_{in} can be calculated as shown in equation (5):

Furthermore, the current value of the excitation circuit is obtained by using (6):

$$I_s = \frac{U_s}{Z_{source} + Z_{in}} \quad (6)$$

Thus, a change of Z_{load} results in a change of Z_{in} , which leads to a change of I_s .

Note that R , $j\omega L$ and $1/j\omega C$ constitute Z_{load} , as shown in equation (7):

$$Z_{load} = R + j\omega L + \frac{1}{j\omega C} \quad (7)$$

For the resistor element, both series compensation and parallel compensation are studied in this paper. The methods are shown in Fig. 4(a) and 4(b), where R' is the compensation resistor, and Z_{load} turns into Z_{load1}' in the case of series compensation, as shown in equation (8):

$$Z_{load1}' = R + j\omega L + \frac{1}{j\omega C} + R' \quad (8)$$

However, Z_{load} turns into Z_{load2}' in the case of parallel compensation, as shown in equation (9):

$$Z_{load2}' = \frac{R R'}{R + R'} + j\omega L + \frac{1}{j\omega C} \quad (9)$$

Where Z_{load1}' and Z_{load2}' represent the equivalent

$$Z_{in} = \frac{U_s - I_s Z_{source}}{I_s} = \frac{Z_s (Z_{load} Z^2 + Z_d Z^2 - Z Z_{34}^2 - Z_{load} Z_{23}^2 - Z_d Z_{23}^2) - Z_{12}^2 (Z Z_{load} + Z Z_d - Z_{34}^2)}{Z (Z Z_{load} + Z Z_d - Z_{34}^2) - Z_{23}^2 (Z_{load} + Z_d)} \quad (5)$$

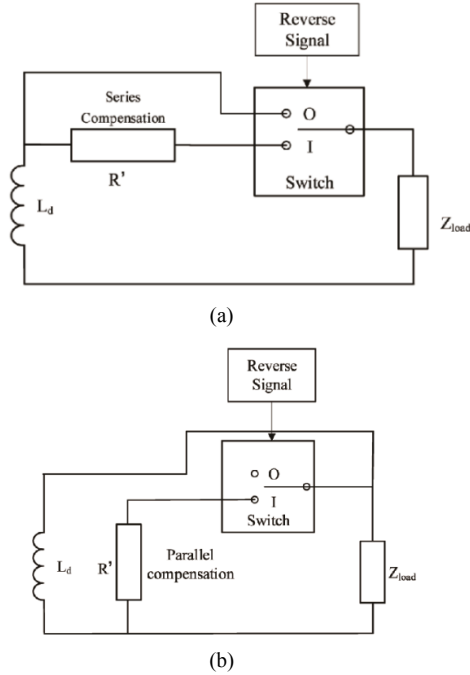


Fig. 4. Compensation circuit diagram. (a) Series compensation circuit. (b) Parallel compensation circuit.

impedances of the load after the compensation resistor is connected.

The network function is expressed as follows:

Where $U_{Z_{load}'}$ represents the voltage of Z_{load}' , and U_{in} represents the voltage of the input impedance Z_{in} .

There are series compensation and parallel compensation for the compensation of the secondary side. Based on equation (10), a Bode diagram is shown in Fig. 5. As can be seen from Fig. 5, $H(j\omega)$ changes both in the parallel compensation and the series compensation. Since the resistor branch is loaded by the switch during signal transmission, it is not easy to ensure the stability of the circuit voltage due to the series resistor loaded in the circuit, which has a negative impact on the stability of the system. Series compensation in the load can result in more obvious voltage gain and phase shift changes. However, a time-domain analysis of the system by Advanced Design System (ADS) software shows that the series form increases the current of the excitation coil, the receiving coil and the coil loss, which reduces the energy transfer efficiency and heats the coil, which is not conducive to the long-term operation of system, as shown in Table I. Therefore, comprehensive consideration, parallel compensation is selected.

Methods for signal modulation and demodulation are mainly amplitude-shift keying (ASK), frequency-shift keying (FSK) and phase-shift keying (PSK). The first two methods

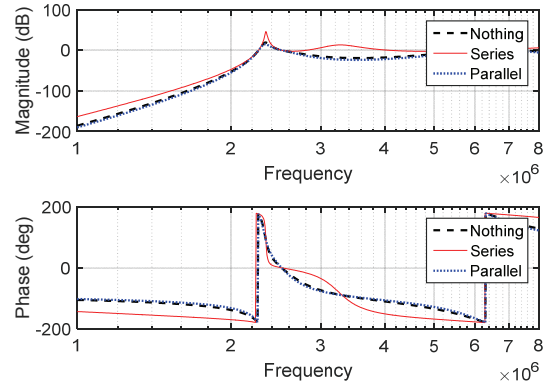


Fig. 5. Bode diagrams of different types of compensation.

TABLE I
SIMULATED CURRENT FOR THE FOUR-COIL STRUCTURE OF
MAGNETICALLY COUPLED RESONANT WIRELESS POWER AND
REVERSE SIGNALS TRANSFER BY ADS

Current	Nothing	Series	Parallel
I_s (A)	3.586	11.931	3.217
I_1 (A)	1.111	1.036	1.114
I_2 (A)	1.060	4.628	0.857
I_d (A)	2.681	2.376	2.699

have little effect on the frequency, and have strong stability. The last method causes a larger frequency change. Thus, PSK cannot be chosen. To ensure that the system operates at the resonance frequency, the best choice is the ASK method, since FSK is a modulation method that uses carrier frequency parameters to carry digital information. Considering the complexity of the transmitter and the receiver, ASK is finally chosen as the method for signal modulation and demodulation in this paper.

In order to simplify the verification of the system, the whole load resistance becomes R_L :

$$R_L = R e \left(\frac{Z_{load} |Z_{23}|^2}{Z_{load}^2 + Z_d^2} \right) \quad (11)$$

Thus, the system efficiency as known as (13):

$$\eta = \frac{P_L}{P_{in}} = \frac{R_L |Z_{23}|^2}{|Z_{23}|^2 (R_2 + R_L) + R_2 (R_2 + R_L)^2} \quad (12)$$

In this paper, a parallel compensation resistor is selected. The R_L changes a system with or without a parallel resistor. It can be seen from equations (11) and (12) that there is a little drop in the system efficiency during signal transmission. In other words, the power gained by the load is slightly decreased by the parallel compensation.

The modulation method is to control the on and off of the

$$H(j\omega) = \frac{U_{Z_{load}'}}{U_{in}} = \frac{Z_{12} Z_{23} Z_{34} Z_{load}'}{Z_s (Z_{load}' Z^2 + Z_d Z^2 - Z_{34}^2 - Z_{load}' Z_{23}^2 - Z_d Z_{23}^2) - Z_{12}^2 (Z Z_{load}' + Z Z_d - Z_{34}^2)} \quad (10)$$

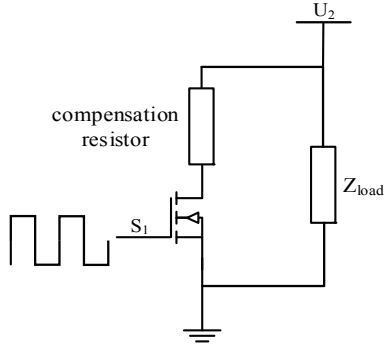


Fig. 6. Circuit of MOSFET switch modulation.

power electronic switches. In this paper, a N-MOSFET is chosen to design the switch circuit for controlling the on and off of the compensation as shown in Fig. 6. When S_1 is turned off, the compensation resistor cannot be incorporated into the circuit. This is the switch off state, which corresponds to the O position of the switch in Fig. 4 (b). In addition, when S_1 is turned on, the compensation resistor can be incorporated into the circuit. This is the switch on state, which corresponds to the I position of the switch in Fig. 4 (b). In this way, signals can be modulated and loaded by controlling the on or off of the MOSFET S_1 . The U_2 in Fig. 6 represents the voltage of the single-turn coil at the receiving end.

When compared with other traditional forms of independent communications, the system makes use of the features of the wireless power transfer system itself. By constantly controlling S_1 according to the data signal, the reverse energy in the wireless power transfer and reverse signals are integrated. The next step is to receive the integrated energy at the transmitting end and demodulate the data.

As for the demodulation method, it is realized as follows. The signals are extracted by the signal extraction coil, and the extracted signals goes through a low pass filter circuit. Most of the high frequency waves can be filtered. After the envelope signals voltage and the reference voltage are compared, the reverse signals are finally obtained. At this point, the complete reverse signal transmission process is completed.

IV. EXPERIMENTS AND RESULTS

In order to demonstrate the effects of different resistances on the reliability of signals, a 3.3MHz resonant frequency with a 100 kHz reverse signals transfer experimental platform was established, as shown in Fig. 7. Wireless power is produced by the RF source and the amplifier. The RF source generates a desired sinusoidal signal. Then the energy of the signal is enlarged by the amplifier. The reverse signals are modulated by the signal load module and they are demodulated by the signal restoration module. The transferred power is metered by a power meter, and it is consumed by coaxial attenuators.

Based on this platform, experiments on different resistances were carried out. The device parameters are listed in Table II.

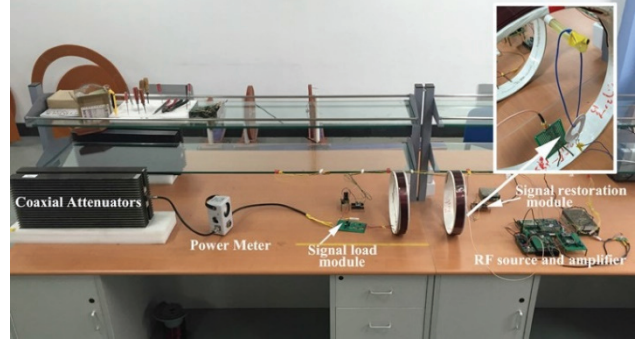


Fig. 7. Experimental platform.

TABLE II
PARAMETERS OF THE FOUR-COIL STRUCTURE OF MAGNETICALLY COUPLED RESONANT WIRELESS POWER AND REVERSE SIGNALS TRANSFER

Parameter	Transmitting Coil	Receiving Coil	Transmitter Resonant Coil	Receiver Resonant Coil	Signal Extraction Coil
$L/\mu\text{H}$	2.9	3	50.2	51.4	25.4
C/pF	703.6	695.2	52.5	51.2	95.4
R/Ω	0.9	0.8	5.1	5.4	4.5
T_{um}	1	1	10	10	10
Wire Diameter /mm	2.1	2.1	2.1	2.1	1
Diameter /cm	17	17	17	17	2.1
Resonant Frequency/ MHz	3.3	3.3	3.3	3.3	3.3

A. Impact of a Parallel Resistor on Power Transfer and Signal Extraction

The resonant frequency of the wireless transfer system is 3.3 MHz at a distance of 40 cm, and the distance of the signal extraction coil is 3 cm away from transmitting coil A. The voltage of the secondary side is 28.4 V and the voltage of the signal extraction coil is 5.31 V without compensation. When the resistance is 150 Ω , the voltage of the signal extraction coil is at the top level. However, the voltage of the secondary side is relatively low, which is harmful to the wireless power transfer. When the resistance is 350 Ω , the voltage of the secondary side is relatively high. However, the voltage of the signal extraction coil is low, which is harmful to the signal extraction. When the resistance is 200 Ω , the voltage of the secondary side is about 25.5V and the voltage of the signal extraction coil is about 7.25 V, which is helpful for both the wireless power transfer and the signal extraction.

When the wireless synchronous transfer of power and reverse signals system is operating, the system parameters measured at different parallel compensation resistances are shown in Fig. 8(b). It can be seen that when the parallel compensation resistor becomes larger, the system efficiency gradually decreases. When $R' \gg R_{load}$, the equivalent

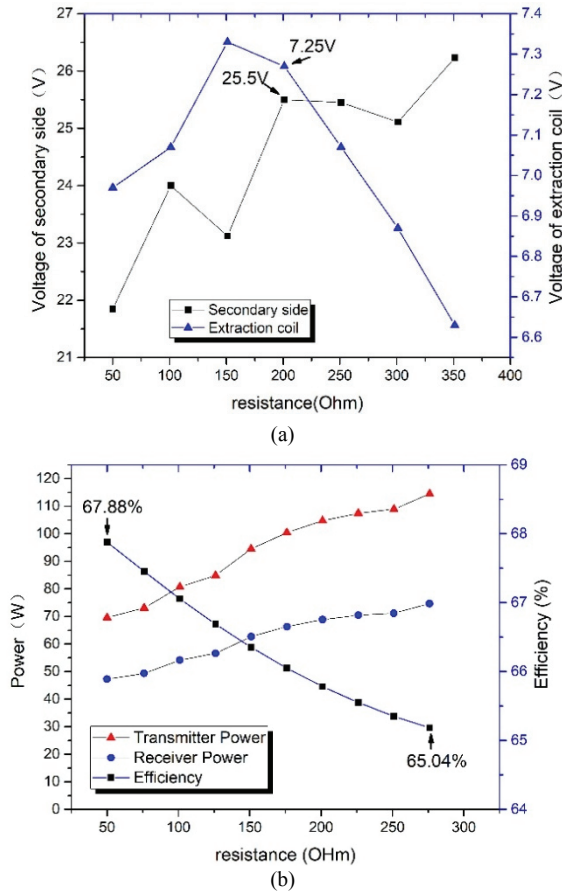


Fig. 8. Results with different resistances. (a) Voltages of the secondary side and the extraction coil. (b) Power and efficiency of the transmitter and receiver.

resistance obtained by connecting two resistors in parallel is approximately equal to R_{load} , and the effect of R' on the power gained by the load is negligible. However, a larger R' results in a stronger thermal effect, which results in a loss of electric energy and harms to the stability of the system. Therefore, a 200Ω resistor was used as compensation in this system.

B. Modulation and Demodulation of Reverse Signals

The frequency of the reverse signal is 100 kHz. An oscilloscope image of the experimental waveforms of the reverse signal and extraction coil are shown in Fig. 9(a). Waveforms of the reverse signal and resonant coil are shown in Fig. 9(b). In both of the figures, the upper waveform represents the high and low levels of the digital signals, while lower waveform is a voltage waveform of the signal extraction coil or resonant coil in different transmitted signals. When the transmitted signal is 1, i.e., it is at a high level and a parallel resistor is connected to the circuit, the primary current and voltage extracted from the signal extraction coil or resonant coil increase. When the transmitted signal is 0, i.e., it is at a low level, the parallel resistor in the circuit is disconnected. Then the primary current and voltage extracted from the

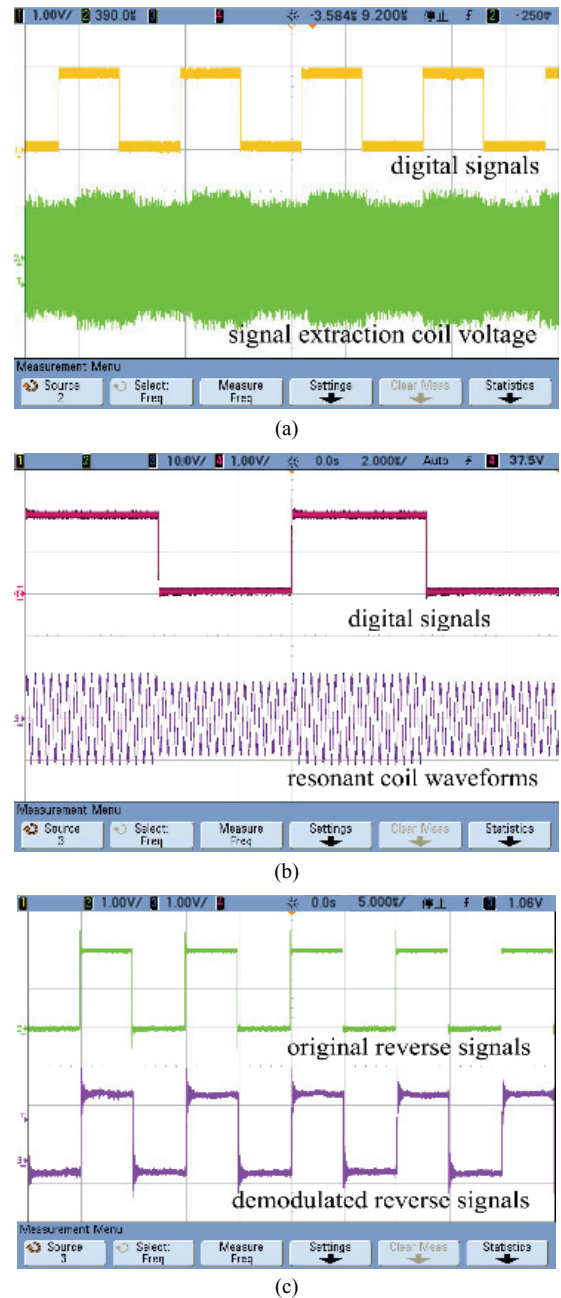


Fig. 9. Oscilloscope images of the modulation and demodulation results. (a) Modulation results. (b) Resonant coil waveforms. (c) Demodulation results.

signal extraction coil or resonant coil decrease.

The power waveform extracted from the signal extraction coil is rebounded by the signal rebounding circuit. Then the initial transmitted electrical level can be obtained. Based on the above experimental platform, the measured experimental waveforms are shown in Fig. 9(c). The top waveform is the original reverse signals, and the lower is the demodulated reverse signals. From the contrast of the high and low electrical levels of the waveform, it can be seen that the change is completely consistent, which means that both the power and reverse signals can be successfully transferred.

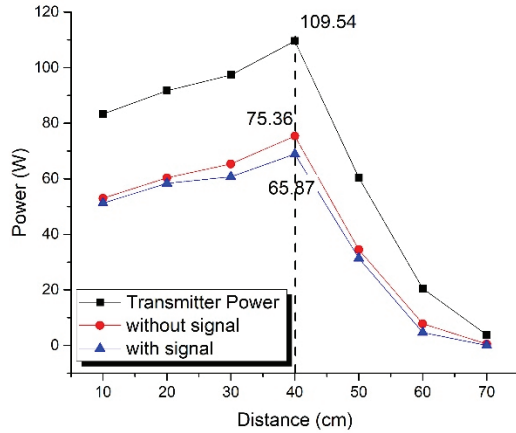


Fig. 10. Experimental results at different distances.

C. Effects of Signal Transmission on Power Transmission

The resonant frequency is 3.3 MHz, and the transmitter power and the receiver power obtained with or without signal transmission at different distances are shown in Fig. 10. When the distance increases, whether there is a loading signal or not, the transmission power increases at first and then decreases. The power is slightly smaller with signal transmission than without signal transmission, which indicates that the signal transmission has a certain but slight effect on the power transmission. It can be seen in Fig. 8(b) and Fig. 10 that a suitable parallel resistance ensures the high efficiency and stability of the system operation.

V. CONCLUSION

In a four-coil wireless power and reverse signals transfer structure, the primary current can be changed by changing the secondary compensation, and the parallel resistor compensation can ensure the stability of the resonant frequency. In addition, the signal loading can be controlled by connecting and disconnecting the parallel resistor. The impedance changes of the secondary side result in changes in the primary current, and these changes can be detected by the signal extraction coil. As a result, the transferred signal can be recovered. The changes in the transmitter power, the receiver power and the efficiency of the system are analyzed while signals are transmitted at different parallel compensations. Furthermore, the distance characteristics of the system are presented.

ACKNOWLEDGMENT

This work was supported by the National Natural Science Foundation of China under Grant [number 51577133], [number 51877151], [number 51607121]; National Key Research and Development Program of China under Grant [number 2017YFB1201003-022]; and Program for Innovative Research Team in University of Tianjin under Grant [number TD13-5040].

REFERENCES

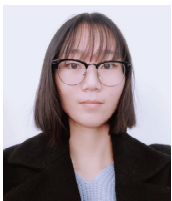
- [1] A. Kurs, A. Karalis, R. Moffatt, J. D. Joannopoulos, P. Fisher, and M. Soljacic, "Wireless power transfer via strongly coupled magnetic resonances," *Science*, Vol. 317, No. 5834, pp. 83-86, Jul. 2007.
- [2] K. A. Karalis, J. D. Joannopoulos, and M. Soljacic, "Efficient wireless non-radiative mid-range energy transfer," *Annals of Physics*, Vol. 323, No. 1, pp. 34-48, Jan. 2008.
- [3] Q.-X. Yang, X. Zhang, Y. Li, G.-Z. Xu, H.-Y. Chen, L.-H. Zhu, Z. Yan, and J. Zhao, *Wireless Power Transmission Technology and its Applications*, 1st ed., China Machine Press, Chapter. 2, pp. 15-26, 2014.
- [4] R. Carta, M. Sfakiotakis, N. Pateromichelakis, J. Thoné, D. P. Tsakiris, and R. Puers, "A multi-coil inductive powering system for an endoscopic capsule with vibratory actuation," *Sensors and Actuators A: Physical*, Vol. 172, No. 1, pp. 253-258, Dec. 2011.
- [5] X.-Y. Liu, F. Zhang, S. A. Hackworth, R. J. Scwabassi, and M. Sun, "Wireless power transfer system design for implanted and worn devices," *2009 IEEE 35th Annual Northeast Bioengineering Conference*, pp. 1-2, 2009.
- [6] Z. Wang, X. Wei, and H. Dai, "Design and control of a 3 kW wireless power transfer system for electric vehicles," *Energies*, Vol. 9, No. 1, pp. 10, Dec. 2015.
- [7] R.-C. Kuo, P. Riehl, A. Satyamoorthy, W. Plumb, P. Tustin, and J.-S. Lin, "A 3D resonant wireless charger for a wearable device and a mobile phone," *2015 IEEE Wireless Power Transfer Conference (WPTC)*, pp. 1-3, 2015.
- [8] X.-Han. Li, H.-R Zhang, F. Peng, Y. Li, T.-Y. Yang, B. Wang, and D.-M. Fang, "A wireless magnetic resonance energy transfer system for micro implantable medical sensors," *Sensors*, Vol. 12, No. 8, pp. 10292-10308, Dec. 2012.
- [9] R. Bansal, "The Future of Wireless Charging [AP-S Turnstile]," *IEEE Antennas and Propagation Magazine*, Vol. 51, No. 2, pp. 153-153, Apr. 2009.
- [10] A. Esser and A. Nagel, "Contactless high speed signal transmission integrated in a compact rotatable power transformer," *European Conference on Power Electronics & Applications*, pp. 409-414, 1993.
- [11] K. Sugano, F. Sato, H. Matsuki, M. Maedako, D. Yoshizawa, T. Sato, and Y. Handa, "A new contactless power-signal transmission device for implanted functional electrical stimulation (FES)," *IEEE Trans. Magn.*, Vol. 40, No. 4, pp. 2964-2966, Aug. 2004.
- [12] Y. Hiraga, J. Hirai, Y. Kaku, Y. Nitta, and K. Ishioka, "Decentralized control of machines with the use of inductive transmission of power and signal," *Industry Applications Society Annual Meeting, Conference Record of the 1994 IEEE*, pp. 875-881, 1994.
- [13] J. Hirai, T.-W. Kim, and A. Kawamura, "Practical study on wireless transmission of power and information for autonomous decentralized manufacturing system," *IEEE Trans. Ind. Electron.*, Vol. 46, No. 2, pp. 349-359, Apr. 1999.
- [14] J. Hirai, T.-W. Kim, and A. Kawamura, "Study on crosstalk in inductive transmission of power and information," *IEEE Trans. Ind. Electron.*, Vol. 46, No. 6, pp. 1174-1182, Dec. 1999.

- [15] J. Hirai, T.-W. Kim, A. Kawamura, "Wireless transmission of power and information and information for cableless linear motor drive," *IEEE Trans. Power Electron.*, Vol. 15, No. 1, pp. 21-27, Jan. 2005.
- [16] J.-F. Zhou, Y. Sun, Y.-G. Su, D. Xin, and Y. Zhai, "Synchronous transmission of inductively coupled power and signal," *Journal of Chongqing Institute of Technology (Natural Science)*, pp. 025, Apr. 2009.
- [17] X. Hao, "Dual-band resonant coupling for simultaneous transmission of power and information," M.S. Thesis, Harbin Institute of Technology, China, 2014.
- [18] C. Wang, "Study on inductively coupled power and data transfer system," M.S. Thesis, Chongqing University, China, 2010.
- [19] S. Fu, "Bidirectional Signal of ICPT system based on frequency and phase modulation," M.S. Thesis, Chongqing University, China, 2014.
- [20] Y. Liu, "Study on signal bidirectional transfer mechanism of ICPT system," M.S. Thesis, Chongqing University, China, 2013.
- [21] W. Tang, R.-X. Yang, Z.-T. Guo, and J.-H. Gu, "Applied research on a high-Q resonant wireless power transmission technology," *Advanced Technology of Electrical Engineering and Energy*, pp. 016, Apr. 2012.



include wireless power transfer and its application.

Yang Li received his B.S., M.S. and Ph.D. degrees in Electrical Engineering from the Hebei University of Technology, Tianjin, China, in 2002, 2005 and 2013, respectively. He is presently working as an Professor in the School of Electrical Engineering and Automation, Tianjin Polytechnic University, Tianjin, China. His current research interests



transfer technology.

Yumei Li was born in Tianjin, China, in 1994. She received her B.S. degree in Electrical Engineering and Automation from the Tianjin Polytechnic University, Tianjin, China, in 2017, where she is presently working towards her M.S. degree in Electrical Engineering. Her current research interests include the electromagnetic field and wireless power



Shaojie Feng was born in Changchun, China. He received his B.S. degree in Electrical Engineering and Automation from the School of Electrical Engineering and Automation, Northeast Electric Power University, Jilin, China, in 2016. He is presently working towards his M.S. degree in Electrical Engineering at the Tianjin Polytechnic University, Tianjin, China. His current research interests include long range and low power wireless power transmission.



Qingxin Yang received his B.S., M.S. and Ph.D. degrees in Electrical Engineering from the Hebei University of Technology, Tianjin, China, in 1983, 1986 and 1997, respectively. He is presently serving as the President of the Tianjin University of Technology, Tianjin, China. His current research interests include electromagnetic field computation and wireless power transfer. Dr. Yang is the President of the China Electrotechnical Society.



Weihao Dong was born in Hebei, China, in 1994. He received his B.S. degree in Electrical Engineering and Automation from the School of Electrical Engineering and Automation, Hebei University of Technology, Tianjin, China, in 2016. He is presently working towards his M.S. degree in Electrical Engineering in the School of Electrical Engineering and Automation, Tianjin Polytechnic University, Tianjin, China. His current research interests include wireless power transfer and its application.



technology.

Jingtai Zhao was born in Shanxi, China, in 1995. He received his B.S. degree in Electrical Engineering and Automation from the Tianjin Polytechnic University, Tianjin, China, in 2017, where he is presently working towards his M.S. degree in Electrical Engineering. His current research interests include the electromagnetic field and power electronics



Ming Xue received his B.S. and M.S. degrees from the Tianjin Polytechnic University, Tianjin, China, in 2011 and 2014, respectively. His current research interests include wireless power transmission.